Special Issue Article

Institution of MECHANICAL ENGINEERS
Journal of POWER AND ENERGY

Proc IMechE Part A:
J Power and Energy
227(6) 637–645

DOI: 10.1177/0957650913499565
pia.sagepub.com
SAGE

Performance improvement of a radial organic Rankine cycle turbine by means of automated computational fluid dynamic design

John Harinck[1], David Pasquale[2], Rene Pecnik[1], Jos van Buijtenen[3] and Piero Colonna[1]

Abstract

There is a growing interest in organic Rankine cycle turbogenerators because of their ability to efficiently utilize external heat sources at low-to-medium temperature in the small-to-medium power range. High-temperature organic Rankine cycle turbines typically operate at very high pressure ratio and expand the organic working fluid in the dense-vapour thermodynamic region, thus requiring computational fluid dynamics solvers coupled with accurate thermodynamic models for their performance assessment and design. In this article we present a steady-state three-dimensional viscous computational fluid dynamics study of the Tri-O-Gen organic Rankine cycle radial turbine, including the radial nozzle, the rotor and the diffuser. The turbine operates with toluene as the working fluid, whose accurate thermophysical properties are obtained with a look-up table approach. Based on the three-dimensional simulation results, together with a two-dimensional fluid dynamic optimisation procedure documented elsewhere, an improved nozzle geometry is designed, manufactured and experimentally tested. Measurements show it delivers 5 kW_e or 4% more net power output, as well as improved off-design performance.

Keywords

Organic Rankine cycle, thermodynamics, real gas, radial turbine, supersonic, nozzle, optimisation, computational fluid dynamics

Date received: 26 June 2013; accepted: 28 June 2013

Introduction

Background

Organic Rankine cycles (ORC) operate using an organic working fluid, which allows for the efficient application of the Rankine cycle principle for the energy conversion of low-temperature heat sources (starting from approximately 90°C) and for low-power output (from few kW_e up to few MW_e). Steam turbines in the low power range cannot reach the same level of efficiency of ORC turbines with the same level of technology. The optimal design of a steam turbine for such a low power range requires many stages, small blade dimensions and very high rotational speeds, which in turn may lead to severe penalties on the efficiency. On the contrary, a turbine operated with an organic fluid can reach very high isentropic efficiency with just one or two stages often rotating at a much lower speed.

Current applications of ORC turbogenerators include the electricity generation from low-grade geothermal heat reservoirs, from biomass fuel and the energy recovery from gas turbines or reciprocating engines and from industrial waste heat. The installed power of geothermal ORC plants totals more than 1000 MW_e[1] and can be considered a mature technology.[2] ORC systems designed for comparatively high-temperature heat sources have been demonstrated to

[1]Delft University of Technology, Faculty of Mechanical Engineering, Maritime and Materials Engineering, Delft, The Netherlands
[2]Università degli Studi di Brescia, Dipartimento di Ingegneria Meccanica e Industriale, Brescia, Italy
[3]Tri-O-Gen B.V., Goor, The Netherlands

Corresponding author:
John Harinck, Delft University of Technology, Faculty of Mechanical Engineering, Maritime and Materials Engineering, Leeghwaterstraat 44, Delft 2628 CA, The Netherlands.
Email: j.harinck@tudelft.nl

be a viable technology for small-scale biomass-fired combined heat and power energy conversion.[3–5]

It can be shown that with the heat of vaporization of organic fluids being much lower than that of water, a better match between the heating trajectory of the working fluid and the cooling trajectory of the heat source can be achieved. As a result, the heat source can be cooled to a significantly lower temperature.[6] The selection of the working fluid is also key to the achievement of a high isentropic efficiency of the turboexpander,[7–10] which is usually single-stage and often features a low peripheral speed and optimal dimensions.

Compared with steam and gas turbines, the expansion in ORC turbines has two distinguishing characteristics. Due to the use of heavy and molecularly complex organic substances as working fluids, the expansion features a comparatively smaller specific enthalpy drop, which allows for the adoption of only one or two stages, without running into the problem of high rotational speed and associated penalties on efficiency.[7] As a result though, the expansion pressure ratio per stage is typically very high (5–50), especially for radial turbines (50–150), so that the flow through the stator nozzle is highly supersonic. The second important difference is the fact that the initial part of the expansion process takes place comparatively close to the critical point of the working fluid, in the so-called dense-gas or real-gas thermodynamic region, where the ideal gas law is not applicable. Complex thermodynamic models of organic fluids are therefore required for the correct and accurate (computational) fluid dynamic design and performance evaluation of high-expansion ratio ORC turbines.

Motivation

The need for fluid dynamic simulations of expansions in the dense-gas region has led to the interfacing of existing finite-volume computational fluid dynamics (CFD) solvers with programs for the estimation of thermodynamic properties of fluids, featuring various degrees of accuracy.[11–20] Examples of such CFD programs are the zFlow solver[18] and the Finflo solver, which was extended to allow for real-gas simulations[12] in order to aid the aerodynamic design of the stator of an ORC turbine.[21] The commercial CFD codes ANSYS CFX and Fluent can also be interfaced with real-gas thermodynamic property tables and models, respectively.[22,23]

Methods for the fluid dynamic design of turbines have become increasingly more sophisticated and their use is facilitated by the constant increase in computational power. Many existing and currently operational ORC turbines have been designed using quasi one-dimensional inviscid or two-dimensional (2D) viscous flow solvers coupled to thermodynamic models that at the time were the most accurate.[13,21] These methods have been used only for the design of the stator, as it is typically the only part that expands partially in the dense-vapour thermodynamic region. Nowadays, similar to what is common practice for the design of steam and gas turbines, the fluid dynamic design of ORC turbines can be accomplished with sophisticated computational methods. For example, it is possible to perform three-dimensional (3D) turbulent Reynolds-Averaged Navier-Stokes (RANS) simulations of the complete turbine coupled with highly accurate multi-parameter equations of state. These methods potentially allow for more accurate results and for more insight into the fluid dynamic performance of the machine and, consequentially, into areas for possible improvement. Even more, state-of-the-art mathematical optimisation methods can now be applied to automatically design the optimal aerodynamic shape, given an appropriate objective function, thus assisting or replacing the traditional trial-and-error procedure.

Goal

First, the study documented here aims to demonstrate the possibility of effectively simulating large pressure-ratio dense-vapour flows through a complete radial ORC turbine using state-of-the-art models. The second objective is to assess with upgraded models the fluid dynamic performance of the stator, which was designed more than a decade ago using tools available of that time. Third, and most importantly, it presents a brief discussion of one of the design improvements that has been implemented based on CFD results and optimisation.

The Tri-O-Gen radial ORC turbine

The turbine flow under investigation is that of the 165 kWe ORC turbogenerator manufactured by Tri-O-Gen B.V. in the Netherlands, which is typically used to recover waste heat from biogas engines or landfill gas.[21] It features a new turbo-generator concept, using toluene as a working fluid. Liquid toluene is also used for lubrication of the shaft bearings. This concept allows for a completely hermetic design, with no need for shaft seals or a separate lubrication system. The turbine and main pump of this ORC system are mounted on the same shaft, together with the high-speed electrical generator, shown in Figure 1.

The single-stage turbine consists of a supersonic nozzle row, arranged around the circumference of a radial-inflow rotor, with only radial low-reaction blading and no axial exducer. This turbine features a very high pressure ratio and specific power, even compared with other ORC turbines. The original aerodynamic design of the Tri-O-Gen turbine was performed at the Lappeenranta University of Technology in Finland using the turbulent RANS Finflo flow solver,[13,21] which, for the flow simulation

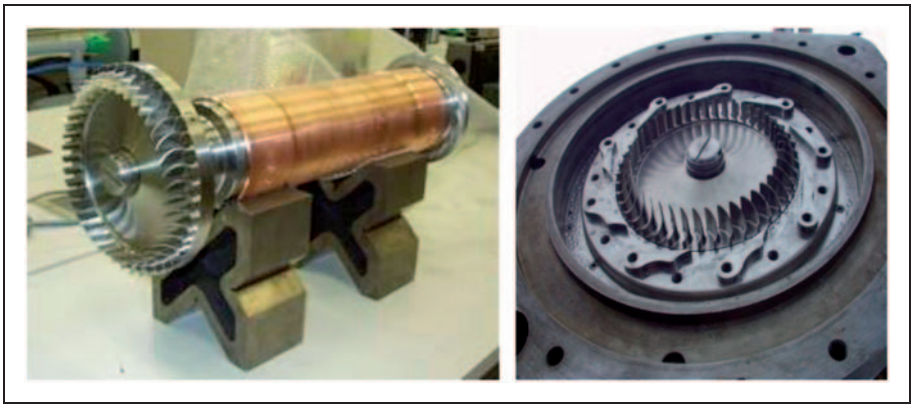

Figure 1. The rotor and generator of the Tri-O-Gen ORC turbogenerator (left) and the rotor and one half of the stator nozzle ring (right).

of the stator, had been interfaced with thermodynamic property data of toluene based on a thermodynamic model developed by Goodwin, which at the time was the most accurate thermodynamic model available for toluene.[24] The CFD analysis of the stator design was based on a 2D single-block structured grid containing 128 cells in the flow direction and 64 cells across it.

Methodology

Approach

In order to evaluate in more detail the flow field and performance of the turbine, and in particular of the stator nozzle, numerical flow simulations were carried out using state-of-the-art models. Due to the supersonic flow, shock losses were expected. Preliminary 2D simulations of the stator nozzle were first carried out based on an assumed value for the back-pressure. Although the flow in the divergent part of the stator is entirely supersonic, it is subsonic in the radial direction, so that the back-pressure affects the flow field solution. Notwithstanding several attempts made in the past to measure the stator back-pressure, an accurate value of the pressure at the nozzle outlet was not known. For this reason, it was decided to simulate the flow path throughout the complete turbine, i.e. stator, rotor and diffuser. This would also provide the best possible estimation of the stator back-pressure, a value of paramount importance for the planned stator nozzle fluid dynamic optimisation.

Viscous simulations of the entire turbine flow were performed for various turbine operating conditions, which were obtained from measurements. In all cases, the flow in the turbine was assumed to be adiabatic and steady state. In reality, some degree of thermal loss can be expected from the high-temperature turbine, through the turbogenerator casing, to the low-temperature pump and surroundings. Moreover, the real flow is unsteady due to rotor–stator interaction: the rotor blades are affected by the periodic interaction with the turbulent wakes and shock waves caused by the stator, leading to flow angle and velocity variations. The adiabatic and steady flow assumptions are often adopted for fluid dynamic simulations aimed at the design and assessment of turbomachinery, as they do not affect the main flow features.

Models

The 3D finite volume RANS solver implemented in a commercial CFD tool was adopted to simulate the adiabatic steady-state flow.[25] The Shear Stress Transport k-ω turbulence model[26,27] was selected for the turbulent transport, as it is known to give good predictions in regions of adverse pressure gradients and separating flow. The chosen CFD solver has been validated by comparison with accurate experimental data related to numerous flows occurring in the ideal-gas thermodynamic region and for geometries similar to the one considered here.

The inlet conditions of the Tri-O-Gen turbine are in the dense-gas thermodynamic region, as indicated by the value of the compressibility factor of $Z_1 = 0.6$. The thermo-physical properties of toluene are therefore obtained via a look-up table procedure. Toluene property data were generated with the multi-parameter equation of state developed by Lemmon and Span[28] and implemented in a commercial program for fluid thermophysical properties estimation.[29] The multi-parameter equation of state is highly accurate, as evidenced by the low uncertainties in the relevant vapour-phase properties documented in the study by Lemmon and Span.[28] The values of the properties specific enthalpy, sound speed, specific volume, isochoric heat capacity, isobaric heat capacity, $[\partial P/\partial v]_T$, specific entropy, viscosity and thermal conductivity are tabulated for $1 \times 10^{-5} \leqslant P \leqslant 50$ bar and $10 \leqslant T \leqslant 370$°C in 500 and 700 equidistant intervals. This allows for property evaluation also somewhat outside the range of conditions of the expansion, as this is often required in the initial phase of the numerical procedure.

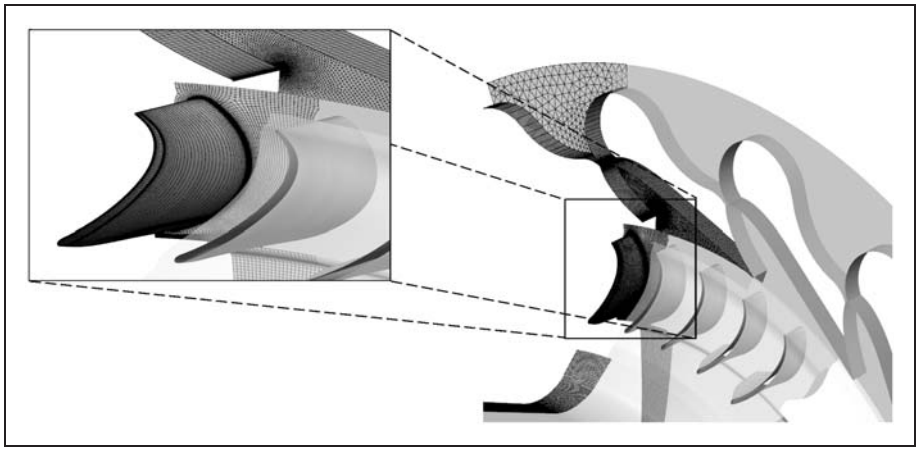

Figure 2. The three-dimensional geometric model with selected surface meshes of the stator, rotor and diffuser meshes.

Due to the lack of measurements of flows occurring in the dense-gas region, CFD codes have not been properly validated by comparison with dense-gas flow measurements. However, here we present a qualitative validation of the solver coupled to the accurate thermo-physical properties model, based on experimental information related to shock wave locations. To the knowledge of the authors, this is an original scientific result.

Mesh generation and domain interfaces

Three-dimensional structured viscous computational meshes were generated for the stator, rotor and diffuser, consisting of 762,960, 600,831 and 565,136 hexahedral and wedge cells, respectively. Selected surfaces of the meshes are shown, in a slightly modified form to respect the confidentiality of the design in Figure 2. The grids were generated such that the non-dimensional wall distance y^+ is of order 1 or smaller at the first cell adjacent to the wall. The rotor blade leading edge is located very close to the leading edge of the rotating hub. In order to avoid computational problems, the rotating mesh representing the rotor was generated with a slightly larger diameter than the real rotor hub. A mixing plane (stage) interface and frozen rotor interface are used for the interfaces between stator–rotor and rotor–diffuser, respectively.

Boundary conditions

The boundary conditions are specified in Table 1. An extension of two times the diffuser diameter and a radial-equilibrium pressure distribution along the outlet boundary were used in order to eliminate possible adverse effects.

Convergence criteria

The convergence of the simulations was ensured by monitoring the residuals and the maximum change in pseudo-time of the mass flow entering and leaving the computational domain. The iterations were continued until the scaled residuals had decreased at least five orders in magnitude for all the conserved quantities. For these values of the residuals, the difference in mass flow rate was smaller than 0.5%.

Simulation results

Stator flow

The original stator was designed to expand the flow to supersonic velocities and give it a very high tangential component before it enters the rotor. An example of the computed flow field solution is presented in Figure 3 (left), in a slightly modified form for reasons of confidentiality. Due to the high pressure ratio and low-reaction blading, the flow passing through the stator nozzles expands to supersonic velocities of approximately $Ma_2 = 2.6$. As the flow enters the mixing region, i.e. the region between the nozzle trailing edge and the rotor inlet, it can no longer maintain its direction due to the flow coming from the adjacent stator nozzle at a different angle. At the trailing edge, the two flows collide and the flow is turned into itself, which, at supersonic velocities, leads to the formation of an oblique shock wave emerging from the trailing edge of the stator nozzle. Black deposit on the endwall of the stator nozzle (as generated for flow visualization), as also shown in Figure 3 (right), appears to support the location of the shock wave and the presence of this flow structure. The oblique shock wave is reflected from the opposite stator-vane wall towards the outlet of the computational domain and the turbine rotor inlet. The flow structure is typical of radial high-expansion ratio turbines.

The oblique shock wave and its reflection cause the flow to change its flow angle. This leads to a non-uniform flow angle along the stator exit–rotor inlet interface. As can be observed in Figure 4(a), the resulting variation in the absolute flow angle is appreciable (9°); however, for the relative rotor inlet angle, shown in Figure 4(b), the variation becomes very

Table 1. The boundary conditions used for the simulation.

Location	Type	Value
Stator inlet	Total pressure, P_{01} (bar)	32.1
Stator inlet	Total temperature, T_{01} (°C)	317
Stator–rotor interface	Mixing plane (stage)	-
Rotor domain	Rotational speed, N (Hz)	430
Rotor–diffuser interface	Frozen rotor	-
Diffuser outlet	Static pressure, P_4 (bar), with radial equilibrium	0.292

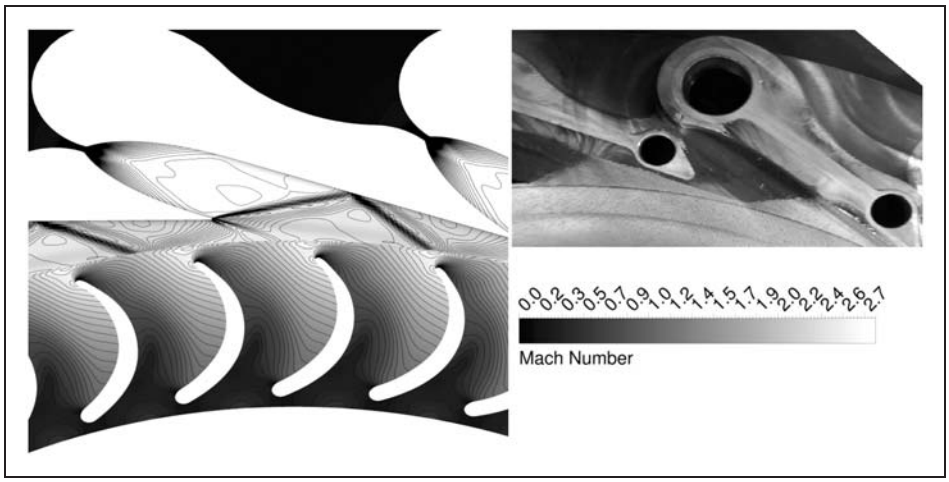

Figure 3. Comparison of Mach number distribution with pressure contours in stator and pressure distribution in rotor at midspan (left); photo of the stator after operation at a similar pressure ratio, with black deposit indicating the location of the shock wave (right).

large (20°). A similarly large variation can be expected for the rotor incidence. A variation of approximately 20° in incidence, around a certain low optimal average positive incidence, is likely to lead to zero or negative incidence on one extreme and >20° incidence, meaning a high risk of stall,[30] on the other extreme. Notwithstanding the fact that there is likely to be insufficient time for the flow to completely settle at the extremes, the flow field around the rotor blades is likely to continuously fluctuate between no (or even negative) blade loading and flow separation (stall) and therefore sub-optimal blade loading.

The loading and risk of flow separation at these two extremes are further amplified by the relative inlet velocity, which is not so much affected by the shocks but more so by the turbulent wake of the stator vane. This leads to a near 25% variation in relative flow velocity with respect to the average value (Figure 4(d)), with the low velocity extreme coinciding with low-to-negative incidence and the high velocity extreme coinciding with excessively high incidence. Similar variations can be observed for the absolute and relative Mach number at rotor inlet in Figure 4(e) and (f). These large variations in relative flow angle and relative velocity lead to a sub-optimal flow situation and rotor power output.

Optimisation of stator for uniform outflow

Based on the flow simulation results, there appeared to be room for performance improvement, in particular with respect to the large variations in stator flow outlet angle and velocity along the circumferential angle. These variations cause even larger variations of approximately 20° in rotor blade incidence and 25% in relative velocity, with coinciding extremes. This leads to high risks of alternating flow separation and low loading of the rotor and thus to sub-optimal turbine performance. The large flow angle variation is inherently caused by the radial arrangement of nozzles that are linear and are designed without taking into account radial pressure equilibrium.

Possibilities to remedy this defect and to redesign the stator such that it produces a uniform rotor inlet angle and velocity have been considered and range from curving or bending the linear stator nozzles to adopting a smaller stator trailing edge angle. However, this type of flow geometry refinement is very difficult to realize using analytical methods and, in addition, time consuming if CFD flow simulations are used in a manual trial-and-error approach for design refinement. For these applications, numerical optimisation methods coupled to the CFD flow solver

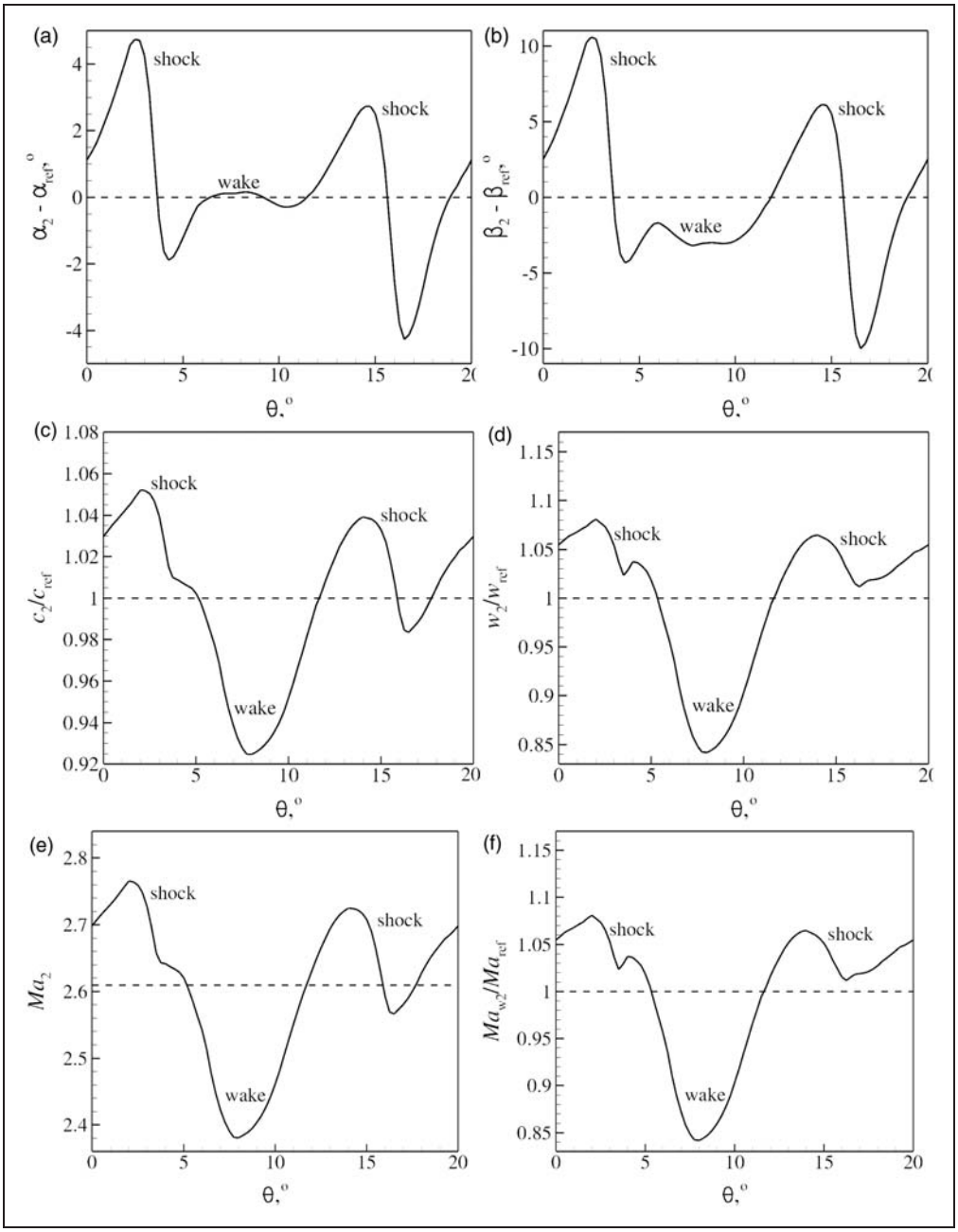

Figure 4. Rotor inlet flow property distributions as a function of the circumferential angle θ for one stator passage at rotor mid-blade span. Except for the absolute Mach number, all properties are non-dimensionalised with respect to their average value. Flow angles α and β are measured with respect to the radial direction.

and approximate meta-models offer a viable solution.[31]

A numerical optimisation system for 2D radial nozzles was therefore proposed and used to optimise the stator geometry for outflow conditions as uniform as possible. The optimisation was performed by means of an in-house CFD code performing inviscid 2D simulations,[18] a genetic algorithm and a meta-model, as documented in more detail in the study by Pasquale et al.[32]

The results from the 3D CFD simulation could not be used directly as target conditions for the 2D optimisation for the following two reasons. First, the radius of the stator outlet used in the 2D domain optimisation was located at 0.94 times the trailing edge radius, which is at a lower radius than the real outflow boundary. This was done in order to avoid the spurious reflection of shocks caused by the implementation of the boundary condition in the 2D solver. Second, being 2D, the domain did not include the small increase in stator height near the stator outlet, corresponding to a 10–12% larger cross-sectional area, which thus significantly affects the flow angle and velocity. By assuming an isentropic expansion/compression in the radial direction and by solving the implicit problem given by the conservation of mass, energy and radial equilibrium, the area-averaged flow properties were extrapolated to smaller

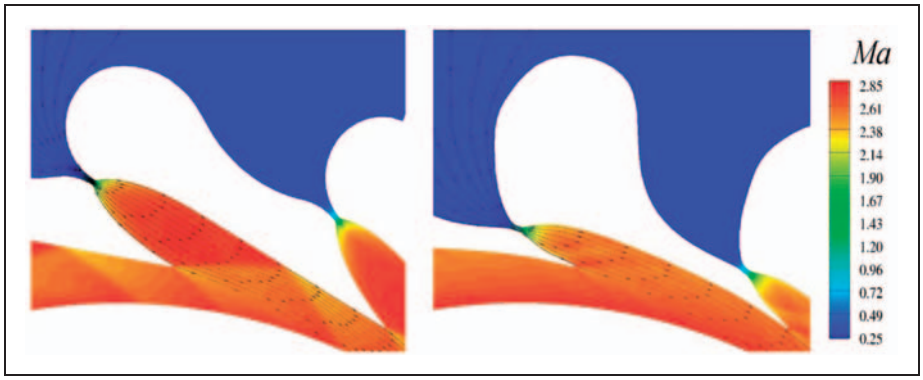

Figure 5. Comparison of the Mach number field between the original (left) and optimised (right) stator geometry simulated in the two-dimensional domain.

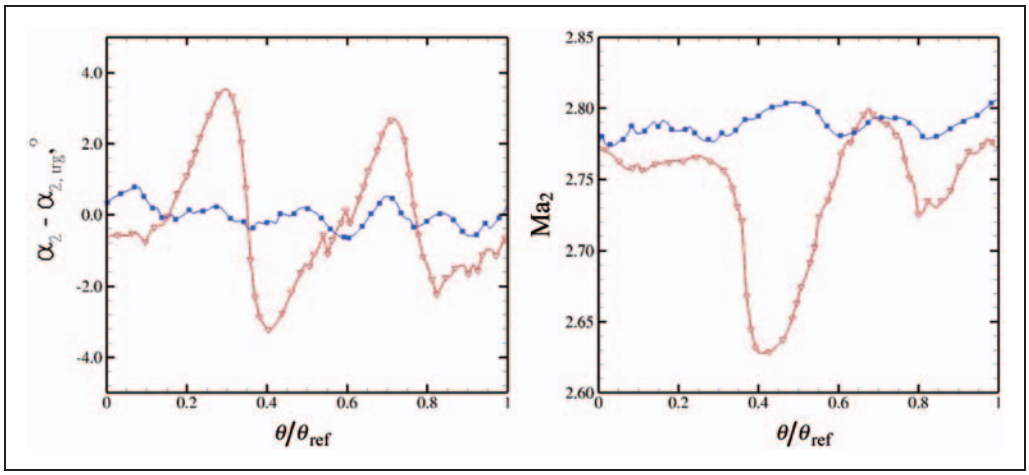

Figure 6. Absolute flow angle (left) and Mach number distribution (right) at stator outlet as a function of the non-dimensionalised circumferential angle for a range corresponding to one nozzle passage. A comparison is made between results for the original (red line with open triangles) and optimised (blue line with closed squares) stator geometry simulated in the two-dimensional domain. The flow angle α is measured with respect to the radial direction.

radii up to the required radius and for constant stator height. The obtained static pressure and flow angle were used as target conditions for the objective function in the stator optimisation, as documented in studies conducted by Pasquale et al.[32,33]

The optimal stator geometry features a curved mean line as expected and 2D simulations indicated it would provide a much more uniform outflow due to the absence of shock waves, as shown in Figure 5 (with modified aspect ratio to respect the confidentiality of the design) and Figure 6. The optimised stator was manufactured and tested in the turbine. Measurements presented in Figure 7 show that the turbine with optimised stator delivers 5 kW_e or 3.5% more net power output and also performs better at off-design operating conditions.

Conclusions

The complete steady-state fluid dynamic simulation of the flow passages, including stator, rotor and diffuser, of the Tri-O-Gen ORC turbine has been successfully performed. Due to the very high pressure ratio and radial arrangement of nozzles featuring a straight mean line, the dense-vapour expansion through the original stator of the turbine was affected by strong oblique shock waves. According to the presented 3D RANS simulations, the shock waves, together with the viscous wake of the blade, create a large variation in flow outlet angle and velocity along the circumference of the rotor inlet. These in turn caused even larger variations of approximately 20° in rotor blade incidence and nearly 25% in relative velocity. Since the extremes in these variations coincide, there was a high risk of alternating flow separation and low loading of the rotor. Although the simulated steady-state adiabatic turbine isentropic efficiency appears to be good, the aforementioned risk indicated a sub-optimal turbine performance that could be improved. The complete steady-state simulation of the flow passages, including stator, rotor and diffuser has been successfully performed.

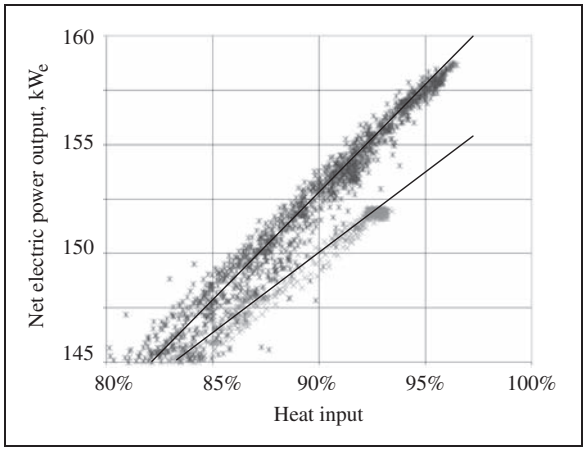

Figure 7. Measurement data of net electric power output as a function of relative heat input for optimised (black symbols) and original stator geometry (grey symbols) and their linear regression lines.

Due to the lack of measurements of flows occurring in the dense-gas region, CFD codes have generally not been properly validated by comparison with dense-gas flow measurements. In this article, however, visual information about oblique shock waves in the stator has been used to provide a qualitative validation of the adopted flow model. To the knowledge of the authors, this is an original scientific result.

A numerical optimisation system for 2D radial nozzles, comprising a 2D CFD in-house code, a genetic algorithm and a meta-model was proposed and used to optimise the stator geometry for outflow conditions as uniform as possible. Operating conditions were provided by experiments, while the nozzle back-pressure was calculated from the results of the turbine simulation. The optimised stator geometry was manufactured and tested. Measurements show that the turbine with optimised stator delivers 5 kW_e or 4% more net power output and also performs better at off-design operating conditions.

Funding

This work has been carried out within the Agentschap NL funded research project EOS UKR number 01003.

Acknowledgements

Tri-O-Gen's permission to publish part of the results is greatly acknowledged. The authors wish to thank Quirijn Eppinga and Stefano Ganassin of Tri-O-Gen B.V. for their contributions during the discussion of the results.

Conflict of interest

None declared.

References

1. Bronicki LY. Organic rankine cycles in geothermal power plants – 25 years of Ormat experience. In: *GRC 2007 annual meeting*, Reno, NV, 30 September–3 October 2007, pp. 499–502.
2. Bronicki LY. Electrical power from moderated temperature geothermal sources with modular mini-power plants. *Geothermics* 1988; 17(1): 83–89.
3. Bini R and Manciana E. Organic Rankine cycle turbogenerators for combined heat and power production from biomass. In: *Proceedings of the 3rd Munich discussion meeting "energy conversion from biomass fuels: current trends and future systems"*, Munich, Germany, 22–23 October 1996, pp. 1–8 and 22–23.
4. Obernberger I, Thonhofer P and Reisenhofer E. Description and evaluation of the new 1000 kW ORC process integrated in the biomass CHP plant in Lienz, Austria. *Euroheat Power* 2002; 10: 1–17.
5. Bini R, Duvia A, Schwarz A, et al. Operational results of the first biomass CHP plant in Italy based on Organic Rankine Cycle turbogenerator and overview of a number of plants in operation in Europe since 1998. In: *Proceedings of 2nd world biomass conference,* Rzym, Poland, 10–14 May 2004, pages 1–6.
6. Larjola J. Electricity from industrial waste heat using high-speed organic Rankine cycle (ORC). *Int J Prod Econ* 1995; 41(1-3): 227–235.
7. Angelino G, Gaia M and Macchi E. A review of Italian activity in the field of Organic Rankine Cycles. In: *VDI Berichte – Proceedings of the international VDI-seminar,* Zurich, Switzerland, 10–12 September 1984, vol. 539, pp. 465–482. VDI: VDI Verlag Düsseldorf.
8. Vernau A. Small high-pressure ratio turbines – supersonic turbines for ORC from 3 kW to 1300 kW. VKI lecture series, 1987.
9. Macchi E and Perdichizzi A. Efficiency prediction for axial-flow turbines operating with nonconventional fluids. *J Eng Power* 1981; 103: 718–724.
10. Drescher U and Brüggemann D. Fluid selection for the organic Rankine cycle (ORC) in biomass power and heat plants. *Appl Therm Eng* 2007; 27: 223–228.
11. Colonna P, Rebay S and Silva S. Computer simulations of dense gas flows using complex equations of state for pure fluids and mixtures and state-of-the-art numerical schemes. Scientific report, Università di Brescia, Brescia, Italy, March 2002.
12. Hoffren J. Adaptation of FINFLO for real gases. Technical report 102, Helsinki University of Technology, Laboratory of Applied Thermodynamics, Helsinki, Finland, 1997.
13. Hoffren J, Talonpoika T, Larjola J, et al. Numerical simulation of real-gas flow in a supersonic turbine nozzle ring. *J Eng Gas Turb Power* 2002; 124(2): 395–403.
14. Turunen-Saaresti T, Tang J and Larjola J. A practical real gas model in CFD. In: Wesseling P, Onate E and Périau J (eds) *European conference on computational fluid dynamics (ECCOMAS CFD 2006),* Egmond aan Zee, The Netherlands, 5–8 September 2006.
15. Boncinelli P, Rubechini F, Arnone A, et al. Real-gas effects in turbomachinery flows – a computational fluid dynamics model for fast computations. *J Turbomach* 2004; 126: 268–276.
16. Cinnella P and Congedo PM. A numerical solver for dense gas flows. In: *34th AIAA fluid dynamics conference and exhibit,* Portland, OR, 28 June–1 July 2004, paper no. AIAA 2004-2137, pp. 1–12.
17. Cinnella P and Congedo PM. Inviscid and viscous aerodynamics of dense gases. *J Fluid Mech* 2007; 580: 179–217.

18. Colonna P and Rebay S. Numerical simulation of dense gas flows on unstructured grids with an implicit high resolution upwind Euler solver. *Int J Numer Meth Fl* 2004; 46(7): 735–765.
19. Colonna P, Harinck J, Rebay S, et al. Real-gas effects in organic Rankine cycle turbine nozzles. *J Propul Power* 2008; 24(2): 282–294.
20. Harinck J, Colonna P, Guardone A, et al. Influence of thermodynamic models in 2D flow simulations of turboexpanders. *J Turbomach* 2010; 132(1): 011001.
21. Van Buijtenen JP, Larjola J, Turunen-Saaresti T, et al. Design and validation of a new high expansion ratio radial turbine for ORC applications. In: *Proceedings of the 5th European conference on turbomachinery, fluid dynamics and thermodynamics*, Prague, Czech Republic, 17–22 March 2003, pp. 1–14.
22. FLUENT Inc. Lebanon, NH. FLUENT 6.3 documentation, 2006.
23. Harinck J, Turunen-Saaresti T, Colonna P, et al. Computational study of a high-expansion ratio radial ORC turbine stator. *J Eng Gas Turbines Power* 2010; 132: 054501.
24. Goodwin RD. Toluene thermophysical properties from 178 to 800 K at pressures to 1000 bar. *J Phys Chem Ref Data* 1989; 18(4): 1565–1636.
25. ANSYS Inc. ANSYS CFX version 13 manual, 2011.
26. Menter FR. Zonal two equation k − ω turbulence models for aerodynamic flows. In: 24th AIAA fluid dynamics conference, Orlando, FL, 6–9 July 1993, paper no. 93-2906.
27. Menter FR, Kuntz M and Langtry R. Ten years of industrial experience with the SST turbulence model. *Turb Heat Mass Trans* 2004; 4: 625–632.
28. Lemmon EW and Span R. Short fundamental equations of state for 20 industrial fluids. *J Chem Eng Data* 2006; 51(3): 785–850.
29. Lemmon EW, Huber ML and McLinden MO. NIST standard reference database 23: reference fluid thermodynamic and transport properties-REFPROP, version 9.1, National Institute of Standards and Technology, Standard Reference Data Program, Gaithersburg, 2013.
30. Whitfield A and Baines NC.. *Design of radial turbomachines*. Essex, UK: Longman Scientific and Technical, 1990.
31. Harinck J, Alsalihi Z, Van Buijtenen JP, et al. Optimization of a 3D radial turbine by means of an improved genetic algorithm. In: *Proceedings of the 6th European conference on turbomachinery, fluid dynamics and thermodynamics,* Lille, France, 7–11 March 2005, pp. 1033–1042.
32. Pasquale D, Ghidoni A and Rebay S. Shape optimization of an ORC radial turbine nozzle. In: *First international seminar on ORC power systems,* Delft, The Netherlands, 22–23 September 2011, pp. 1–22.
33. Pasquale D, Ghidoni A and Rebay S. Shape optimization of an ORC radial turbine nozzle. *J Eng Gas Turbines Power* 2013; 135(4): 042308.

Appendix

Notation

C	absolute flow velocity
k	turbulence kinetic energy
Ma	Mach number
N	rotational speed
P	pressure
R	degree of reaction
T	temperature
v	specific volume
w	relative flow velocity
y	wall distance
Z	compressibility factor
α	absolute flow angle
β	relative flow angle
θ	circumferential angle
ω	specific dissipation

Subscripts

0	total conditions
1	turbine inlet
2	stator outlet
4	diffuser outlet
ref	reference value
trg	target value

Superscripts

$+$	non-dimensional